ACS OMEGA

http://pubs.acs.org/journal/acsodf

Article

Fluctuation in the Sliding Movement of Kinesin-Driven Microtubules Is Regulated Using the Deep-Sea Osmolyte Trimethylamine *N*-Oxide

Arif Md. Rashedul Kabir,*[,§] Tasrina Munmun,[§] Kazuki Sada, and Akira Kakugo*

Cite This: *ACS Omega* 2022, 7, 18597−18604

Read Online

ACCESS | Metrics & More | Article Recommendations | Supporting Information

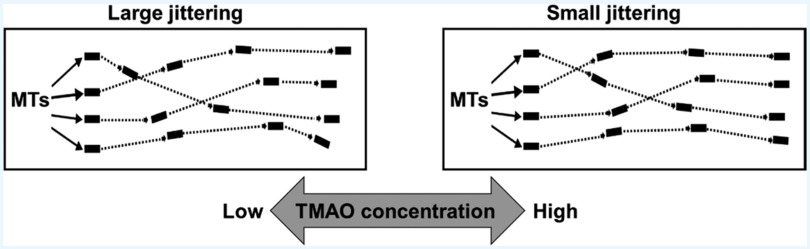

ABSTRACT: Nowadays, biomolecular motor-based miniaturized lab-on-a-chip devices have been attracting much attention for their wide range of nanotechnological applications. Most of the applications are dependent on the motor-driven active transportation of their associated filamentous proteins as shuttles. Fluctuation in the movement of the shuttles is a major contributor to the dispersion in motor-driven active transportation, which limits the efficiency of the miniaturized devices. In this work, by employing the biomolecular motor kinesin and its associated protein filament microtubule as a model active transport system, we demonstrate that the deep-sea osmolyte trimethylamine *N*-oxide (TMAO) is useful in regulating the fluctuation in the motility of microtubule shuttles. We show that the motional diffusion coefficient, a measure of the fluctuation in the movement of the kinesin-propelled microtubules, gradually decreases upon increasing the concentration of TMAO in the transportation system. We have been able to reduce the motional diffusion coefficient of microtubules more than 200 times by employing TMAO at a concentration of 2 M. We also show that upon elimination of TMAO, the motional diffusion coefficient of microtubules can be restored, which confirms that TMAO can be used as a tool to reversibly regulate the fluctuation in the sliding movement of kinesin-propelled microtubule shuttles. Such reversible regulation of the dynamic behavior of the shuttles does not require sacrificing the concentration of fuel used for transportation. Our results confirm the ability to manipulate the nanoscale motion of biomolecular motor-driven active transporters in an artificial environment. This work is expected to further enhance the tunability of biomolecular motor functions, which, in turn, will foster their nanotechnological applications based on active transportation.

1. INTRODUCTION

Biomolecular motors and their associated filamentous proteins play a central role in active transportation of materials in living organisms.[1,2] In cooperation with the associated filamentous proteins, biomolecular motors utilize the chemical energy obtained from hydrolysis of adenosine triphosphate (ATP) and perform mechanical work with remarkably high energy efficiency and specific power.[3] Kinesin is a well-studied biomolecular motor that together with microtubules (MTs) comprise one of the major active transport systems in living organisms, which play pivotal roles in many cellular events.[4] MTs are hollow cylindrical protein filaments formed via polymerization of tubulin heterodimers.[5] In active transportation, MTs serve as the tracks along which kinesins carry cargoes to various locations in cells. The biomolecular motor system MT−kinesin has several attractive features such as nanometer scale, high fuel efficiency, and engineering properties, which motivates its utilization in hybrid micro/nanomechanical devices nowadays.[6−8] *In vitro* gliding assay serves as the platform for most of their applications in artificial environments. In an *in vitro* gliding assay, MTs are propelled on a substrate by surface-adhered kinesins in the presence of ATP. The *in vitro* gliding assay has provided valuable insights into important aspects of biomolecular motor functions.[9−11] Consequently, the MT−kinesin-based active transport system has appeared as a key technology in miniaturized micro/nanodevices for serving various purposes. So far, based on the *in vitro* gliding assay, the MT−kinesin system has been employed in synthetic environments for sensing,[12] nanotransportation and nanostructuring,[13,14] surface imaging,[15] characterizing surface mechanical deformation,[16] force measurement,[17] and molecular robotics.[18]

Received: March 2, 2022
Accepted: May 5, 2022
Published: May 23, 2022

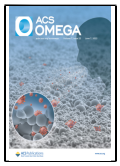

Although the *in vitro* gliding assay has been receiving a great deal of attention as an active transport system, controllability of the motion of shuttles (MTs) has been essential for successful applications of the biomolecular motor-based integrated, hybrid nanodevices. Several reports have attempted to control the functions of biomolecular motors *in vitro* by employing genetic engineering,[19,20] azobenzene-based photoswitches,[21] or tuning physicochemical parameters.[22] However, like any transport system, dispersion is an important metric for biomolecular motor-based active transportation in miniaturized devices.[23] The sensitivity or resolution of any device, based on the active transportation, can be easily affected by the dispersion in transportation. Fluctuation of the velocity of individual transporters, *i.e.*, MTs around their time-average velocity is one of the major contributors to the dispersion in the active transport system constructed from MTs and associated biomolecular motors.[23,24] The motional diffusion coefficient can be employed as a measure of the fluctuation in the velocity of individual shuttles.[23,24] A variation in the velocity of biomolecular motor-driven discrete shuttles along their trajectories may lead to the loss of efficiency; therefore, uniformity in the transportation of the shuttles has been highly desired. However, less attention has been paid to controlling this critical metric of active transportation based on *in vitro* gliding assay. Consequently, there has been no report to guide on how to regulate the fluctuations in the velocity of kinesin-driven microtubule shuttles in an *in vitro* gliding assay. Here, we demonstrate a simple strategy to reversibly regulate the fluctuation of the velocity of kinesin-driven MTs using trimethylamine *N*-oxide (TMAO). TMAO is an osmolyte found in deep-sea animals at high concentrations.[25] TMAO accumulates in the tissue of deep-sea animals and plays protective roles against the protein-destabilizing effects of high temperature, pressure, chemicals, *etc.*[25−27] Nowadays, TMAO is commercially available and it has been employed in artificial environments for stabilizing microtubules[28] and protecting kinesin from thermal denaturation.[29] In this work, using this natural molecule, we show that without sacrificing the concentration of the fuel (ATP) used in the gliding assay system, the fluctuations in the motility of MTs can be regulated over a broad range using TMAO in a concentration-dependent manner. We have performed *in vitro* gliding assay of MTs on kinesins in the presence of a wide range of TMAO concentrations (0−2000 mM), where the concentration of the fuel was kept constant at a saturating level (5 mM). We monitored the motility behavior of the gliding MTs and examined the fluctuations in the movement of the MTs in the presence of various TMAO concentrations by analyzing the mean-square deviation of the sliding displacement of MTs from their average. Moreover, we estimated the motional diffusion coefficient of the kinesin-propelled MTs, which is a measure of the fluctuations in MTs' sliding movement. Our results confirm that TMAO is effective in suppressing the fluctuations in the motility of kinesin-propelled MTs. The motional diffusion coefficient of the gliding MTs decreased upon increasing the TMAO concentration in the gliding assay. We have been able to suppress the motional diffusion coefficient of MTs ∼200-fold by employing 2 M TMAO in the gliding assay. Furthermore, we found that upon elimination of TMAO from the gliding assay, the motional diffusion coefficient of the MTs can be restored to the initial value observed in the absence of TMAO. Therefore, this work offers a facile means to reversibly regulate the fluctuations in the sliding movement of kinesin-propelled MTs in an *in vitro* gliding assay. Such an ability to regulate the dynamic behavior of biomolecular motor-driven shuttles is expected to foster the applications of biomolecular motors and their associated proteins in nanotechnology, material science, and bioengineering.

2. MATERIALS AND METHODS

Chemicals and Buffers. TMAO, purchased from Sigma-Aldrich, was used without further purification. BRB80 buffer was prepared maintaining the final concentration of the components as 80 mM PIPES, 1 mM $MgCl_2$, and 1 mM EGTA. The pH of BRB80 buffer was adjusted to 6.8 using KOH. The BRB80-TMAO imaging solutions contained 5 mM ATP, 1 mM DTT, 2 mM Trolox, 1 mM $MgCl_2$, 10 μM paclitaxel, 0.5 mg/mL casein, 4.5 mg/mL D-glucose, 50 U/mL glucose oxidase, and 50 U/mL catalase.

Purification, Labeling of Tubulin, and Preparation of MTs. Tubulin was purified from the fresh porcine brain using a high-concentration PIPES buffer (1 M PIPES, 20 mM EGTA, 10 mM $MgCl_2$; pH adjusted to 6.8 using KOH) according to a previous report.[30] Atto550-labeled tubulin (RT) was prepared using Atto550 NHS ester (ATTO-TEC, Gmbh) according to a standard technique.[31] The labeling ratio of fluorescence dye to tubulin was ∼1.0, as determined from the absorbance of tubulin at 280 nm and fluorescence dye at 554 nm. MTs were prepared by polymerizing a mixture of RT and nonlabeled tubulin (WT) (RT:WT = 1:1; final tubulin concentration = 40 μM). A total of 4.0 μL of a mixture of RT and WT was mixed with 1 μL of a GTP premix (5 mM GTP, 20 mM $MgCl_2$, 25% DMSO in BRB80) and incubated at 37 °C for 30 min. After polymerization, the MTs were stabilized using paclitaxel (50 μM paclitaxel in DMSO).

Expression and Purification of Motor Protein. A GFP-fused recombinant kinesin-1 construct consisting of the first 465 amino acid residues of human kinesin-1 (K465), an N-terminal histidine tag, and a C-terminal avidin tag was used to propel MTs in the *in vitro* gliding assay. The expression and purification of the kinesin were done as described in a previously published report.[32]

***In Vitro* Gliding Assay.** A flow cell with dimensions of 9 × 2 × 0.1 mm^3 ($L \times W \times H$) was assembled from two cover glasses 9 × 18 mm^2 and 40 × 50 mm^2 (MATSUNAMI) using a double-sided tape as a spacer. First, the flow cell was filled with 5 μL of a 1 mg/mL streptavidin solution (Sigma-Aldrich, S4762) and incubated for 5 min. The flow cell was then washed with wash buffer (80 mM PIPES, 1 mM EGTA, 1 mM $MgCl_2$, and ∼0.5 mg/mL casein; pH 6.8). Next, 5 μL of a kinesin solution (800 nM) was introduced into the streptavidin-coated flow cell. The flow cell was then incubated for 5 min to allow the binding of kinesins to the glass surface through interaction with streptavidin. After washing the flow cell with 10 μL of wash buffer, 10 μL of an MT solution (200 nM, paclitaxel stabilized GTP-MTs) was introduced and incubated for 5 min, which was followed by washing with 10 μL of wash buffer. The motility of the MTs was initiated by applying 5 μL of motility buffer containing 5 mM ATP. In the experiments where TMAO was used, 5 μL of motility buffer containing 5 mM ATP and TMAO of prescribed concentrations was infused into the flow cell. The MTs were monitored using a fluorescence microscope within 5 min of ATP buffer addition. All of the experiments were performed at room temperature (∼22 °C).

https://doi.org/10.1021/acsomega.2c01228
ACS Omega 2022, 7, 18597−18604

Microscopy Image Capture and Data Analysis. Samples were illuminated with a 100 W mercury lamp and visualized using an epi-fluorescence microscope (Eclipse Ti; Nikon) equipped with an oil-coupled Plan Apo 60×1.40 objective (Nikon). A filter block with UV-cut specification (TRITC: EX540/25, DM565, BA606/55; Nikon) was used in the optical path of the microscope that allowed visualization of MTs eliminating the UV part of radiation and minimized the harmful effect of UV radiation on samples. Images were captured using a cooled CMOS camera (Neo CMOS; Andor) connected to a PC. To capture images of MTs for several minutes, an ND4 filter (25% transmittance) was inserted into the illuminating light path of the fluorescence microscope to avoid photobleaching. All movies and images captured using the epi-fluorescence microscope were analyzed using an image analysis software (ImageJ 1.46r).

3. RESULTS AND DISCUSSION

We have explored the effect of TMAO on the sliding movement of kinesin-propelled MTs by performing *in vitro* gliding assay of MTs on a kinesin-coated substrate in which the concentration of TMAO was varied (Figure 1a,b). In brief, a flow cell was prepared on a glass substrate and kinesin motors were adsorbed to the flow cell. MTs, polymerized from tubulin dimers using GTP and stabilized using paclitaxel, were attached to the kinesin-coated surface of the flow cell. The motility of the MTs was initiated by introducing the motility buffer to the flow cell. The concentration of ATP was maintained at a saturating level (5 mM), whereas the concentration of TMAO varied between 0 and 2000 mM. After initiating the motility of MTs, we monitored the gliding MTs using a fluorescence microscope and investigated their motility behavior by examining fluctuations in the movement of individual MTs.

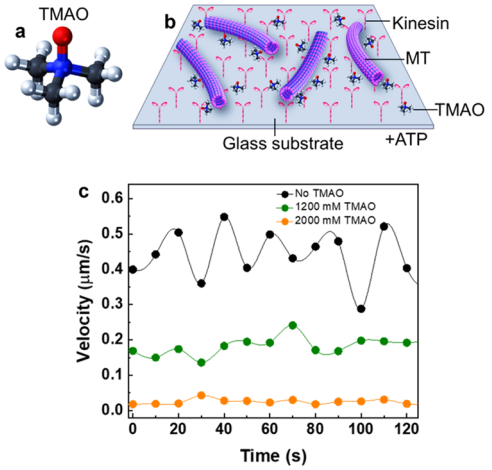

Figure 1. Schematic representation of (a) molecular structure of TMAO and (b) *in vitro* gliding assay of MTs on a kinesin-coated glass substrate in the presence of TMAO. In the molecular structure of TMAO, the red, blue, black, and white spheres denote the oxygen, nitrogen, carbon, and hydrogen atoms, respectively. "+ATP" indicates the use of ATP in the *in vitro* gliding assay. (c) Representative data show the instantaneous velocity of an MT with time where the velocity was quantified over a 10 s interval. Abrupt changes in the velocity of MTs with time were observed in the absence of TMAO, which diminished upon increasing the concentration of TMAO.

First, we examined the instantaneous velocity of the MT filaments along their trajectories. As shown by the representative data in Figure 1c, the instantaneous velocity of a single MT along its gliding trajectory fluctuates frequently when TMAO was not used in the gliding assay (Movie S1). On contrary, in the presence of TMAO (*e.g.*, 1200 mM), such abrupt fluctuations in the instantaneous velocity of MTs seems to be diminished (Movie S2), which could be clearly observed in Figure 1c, when the concentration of TMAO was increased further (*e.g.*, 2000 mM). To confirm the suppression of the fluctuation in MTs' velocity in the presence of TMAO, we plotted the histogram of the instantaneous velocity of MTs over 10 s intervals (Figure 2), where the number of MTs considered was 50 in each condition. In the absence of TMAO, the instantaneous velocity of MTs was found to be distributed over a wide range around the mean value. Upon introducing the TMAO in the gliding assay (*e.g.*, 400 or 800 mM), the range of distribution of the instantaneous velocity of MTs became narrower. The range of the instantaneous velocity of MTs became even smaller upon increasing the TMAO concentration further in the gliding assay (*e.g.*, 1500, 2000 mM). Thus, these results clearly indicate that TMAO affects the dynamic behavior of kinesin-propelled MTs in the gliding assay. It is to note that we also noticed a gradual shift of the histograms of MT velocity toward lower values, which agrees to past reports on kinesin-propelled MTs or myosin-propelled actin filaments.[33,34]

To quantify the TMAO-mediated diminution of the distribution range of MTs' instantaneous velocity, we fitted the histograms according to the equation of Gaussian distribution and estimated the mean and standard deviation in each case. The results, shown in Figure S1, reveal that the standard deviation of MT velocity around the mean decreases upon increasing the TMAO concentration in the gliding assay. A similar trend was observed even when we considered the standard deviation obtained from the arithmetic mean of MT velocity, instead of the standard deviation and the mean estimated from Gaussian fitting (Figure S2). To confirm that the observed behavior is not a measurement artifact related to lower velocities of MTs at higher TMAO concentrations, the standard deviation was plotted as a function of the average velocity of MTs for each TMAO concentration (Figures S1 and S2). The standard deviation around the mean velocity of MTs was found to change nonlinearly with MT velocity, which suggests that the narrowing of the distribution range of the instantaneous velocity of MTs is due to the presence of TMAO in the gliding assay, not due to the reduction in MT velocity.

To gain a deeper insight into the dynamic behavior of MTs in the presence of varying concentrations of TMAO, we examined the fluctuations in the movement of individual MTs. We calculated the mean-square deviation of the sliding displacement of MTs from the average with averaging of multiple trajectories,[23,24,35] which when plotted as a function of time produces a diffusion coefficient of the motile MTs according to the following equation

$$<(\Delta X_{v-flu})^2> = 2D_{v-flu}\cdot t$$

Here, $<(\Delta X_{v\text{-}flu})^2> = <(\Delta X(t) - v\Delta t)^2>$, where $X(t)$ is the position of MT filaments along their trajectories, $\Delta X(t) = X(t + \Delta t) - X(t)$ is the displacement of the filaments during time Δt, "v" is the mean velocity of MTs, and $D_{v\text{-}flu}$ is the diffusion coefficient of MTs, which is termed in the literature as the motional diffusion coefficient,[23,24] and is a measure of the

https://doi.org/10.1021/acsomega.2c01228
ACS Omega 2022, 7, 18597−18604

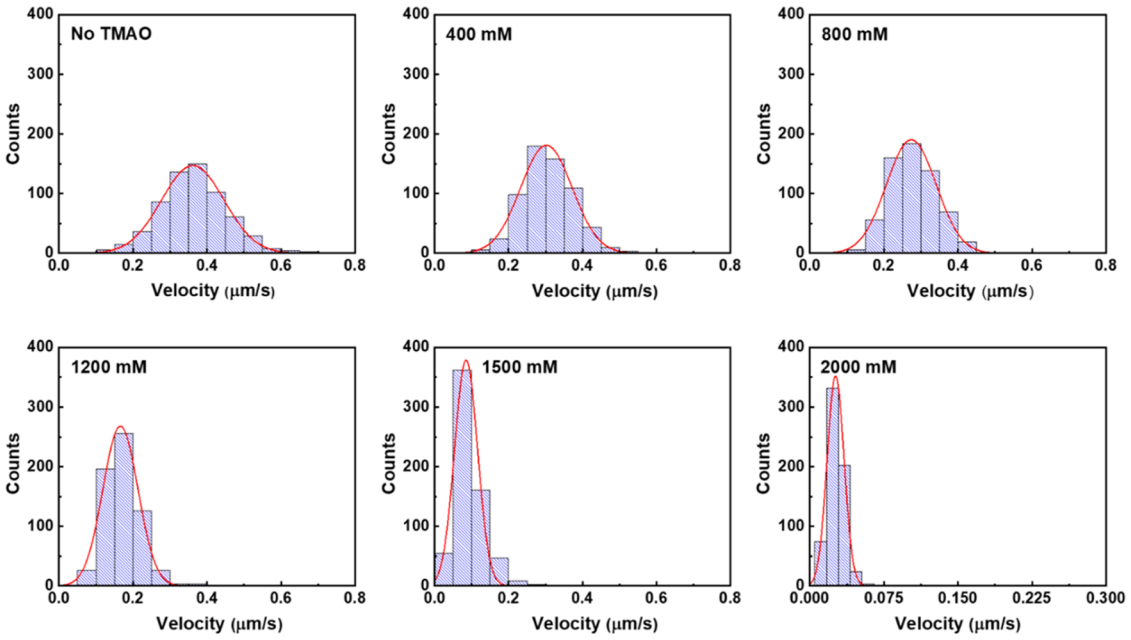

Figure 2. Histograms show the distribution of the instantaneous velocity of MTs in the absence and in the presence of TMAO of various concentrations. The concentration of TMAO is mentioned inside the histograms in each case, and "no TMAO" indicates the absence of TMAO. As the concentration of TMAO in the gliding assay was increased, the histograms became narrower and shifted toward lower velocity values. The red lines represent the fitting of the histograms using the equation of Gaussian distribution.

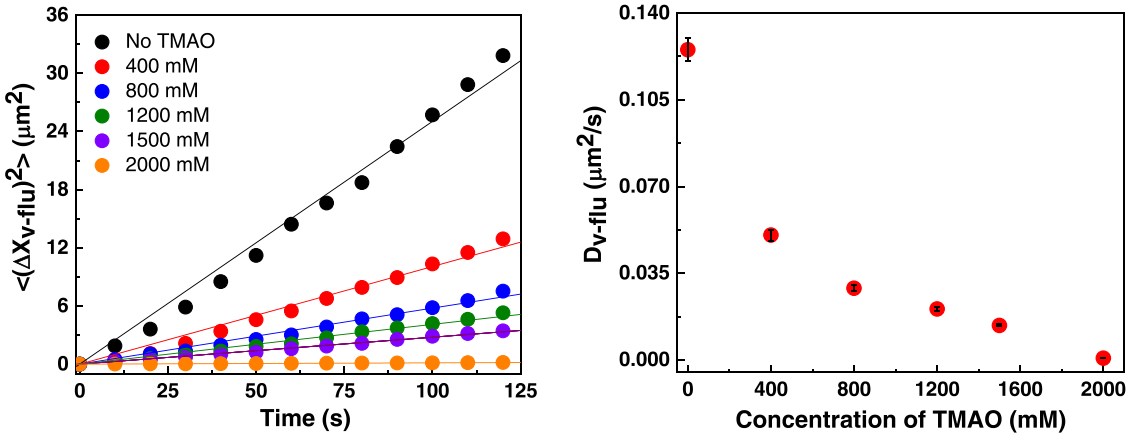

Figure 3. Mean-square displacement deviation of MTs from the average as a function of time, calculated by "multiple trajectories averaging" over 50 different trajectories of MTs, in the absence and in the presence of different TMAO concentrations. Error bars are not shown here for simplicity. The solid lines indicate the linear regression fit of the data in each condition (left). Change in the motional diffusion coefficient of MTs, propelled by kinesins in an *in vitro* gliding assay, upon changing the TMAO concentration in the gliding assay (right). Error bar: standard deviation.

fluctuations of the sliding movement of MTs propelled by kinesin motors. In calculating the mean-square deviation of the sliding displacement of MTs from the average, we ignored short MTs and considered only the relatively long MTs with a length of >15 μm. This is because the motional diffusion coefficient of such long MTs is independent of their length and in-feed kinesin concentration in the gliding assay.[24] As shown in Figure 3, the mean-square displacement deviation from the average increases linearly with time both in the absence and in the presence of TMAO of various concentrations. In this figure, the solid lines for each data set represent the regression line and the motional diffusion coefficient of MTs is estimated as 0.5 times of the slope of these lines. Our results reveal that the motional diffusion coefficient of MTs gradually decreased with increasing the concentration of TMAO in the gliding assay (Figure 3). The motional diffusion coefficient of MTs was 0.125 $\pm$ 0.0047 μm^2 /s in the absence of TMAO, which dropped to $6.7 \times 10^{-4} \pm 2.2 \times 10^{-5}$ μm^2 /s when 2000 mM TMAO was used. This result confirms that fluctuation in MT velocity has been suppressed by more than 200-fold using TMAO in the gliding assay.

Thus, based on these results, it can be confirmed that fluctuations in the sliding movement of MTs are modulated using TMAO in an *in vitro* gliding assay. From our results, it appears that TMAO suppresses both the velocity of MTs and dispersion in MT velocity. Using TMAO, the uniform motion of MTs seems to be achieved at the expense of their suppressed motion. However, the advantage of using TMAO is that we do not need to decrease the ATP concentration or alter other physicochemical parameters to lower the MT velocity or suppress the dispersion of MT velocity. In addition, we have performed further experiments to confirm whether

https://doi.org/10.1021/acsomega.2c01228
ACS Omega 2022, 7, 18597−18604

TMAO plays any direct role in ensuring the uniform motion of MTs. We demonstrated *in vitro* gliding assay of MTs, in the absence of TMAO, by decreasing the ATP concentration from 5 mM to 50 μM. The average velocity of MTs was 106 ± 18 nm/s using 50 μM ATP, which is close to the velocity of MTs (116 ± 16 nm/s) observed using 1000 mM TMAO and 5 mM ATP. In these conditions, the motional diffusion coefficients of MTs were estimated to be 0.032 ± 0.002 and 0.021 ± 0.001 $\mu m^2/s$ when the average MT velocities were 106 ± 18 nm/s (50 μM ATP, no TMAO) and 116 ± 16 nm/s (5 mM ATP, 1000 mM TMAO), respectively. This result clearly reveals that TMAO plays a direct role as a regulator of dispersion in MT velocity.

According to the literature, TMAO can suppress the motility of kinesin-propelled MTs and myosin-driven actin filaments.[33,34] In these works, the motility of MTs or actin filaments was characterized as the time-average velocity of ensembles, which kept the motility behavior of individual shuttles concealed. Furthermore, any effect of TMAO on the fluctuation in velocity of individual MTs was not investigated in these past works, which has been unraveled by the above results. Recently, the use of TMAO also enabled the regulation of MT motility in a reversible manner.[33] Therefore, we have been motivated to investigate if the fluctuation in velocity of individual MTs can also be reversibly regulated using TMAO. To examine, first we performed a gliding assay of MTs on kinesins in the absence of TMAO; then, we applied 1000 mM TMAO in the flow cell by mixing with ATP buffer. Next, by extensive washing of the flow cell, we eliminated the TMAO from the gliding assay. Our results reveal that upon application of 1000 mM TMAO, the range of distribution of the instantaneous velocity of MTs became narrower, which returned to the initial broader range after elimination of the TMAO from the gliding assay (Figure 4). In each condition, we analyzed the mean-square deviation of MT displacement from the average displacement with "multiple trajectory averaging" (Figure 5), based on which we could also confirm the reversibility. Initially, the motional diffusion coefficient of MTs was 0.13 ± 0.002 $\mu m^2/s$ in the absence of TMAO, which was reduced to 0.02 ± 0.0006 $\mu m^2/s$ using 1000 mM TMAO. After the elimination of TMAO, the motional diffusion coefficient of MTs was returned to 0.12 ± 0.002 $\mu m^2/s$ (Figure 5). Such reversible regulation of the fluctuations in MT motility using TMAO coincides with the reversible regulation of the activity of kinesins using TMAO.[33] Overall, these results confirm that the utilization of TMAO offers a simple means to regulate the fluctuations in the sliding movement of kinesin-propelled MTs in a reversible manner.

The motional diffusion coefficient of biomolecular motor-driven MTs is contributed by two factors: thermally generated fluctuations of MT filaments and fluctuations in active force of the kinesin motors. The motional diffusion coefficient is helpful in predicting friction between MTs and kinesin motors. A large value of diffusion coefficient indicates a small friction force between MTs and motors.[24] The observed decrease in the motional diffusion coefficient of the MTs, in the presence of TMAO, suggests higher friction between MTs and kinesins.[24] Such an increase in friction between shuttles and motor proteins may work as a velocity-limiting factor for the shuttles[36] or motors.[37] Decrease in MT velocity upon increasing the TMAO concentration in the gliding assay[33,38] could be accounted for by such an increase in friction between MTs and kinesins mediated by TMAO. Friction between MTs and kinesins may increase when the transition between mechanical states of kinesin is suppressed.[37] Future investigations are required to understand the effect of TMAO on the mechanochemical cycles and energy efficiency of kinesins.

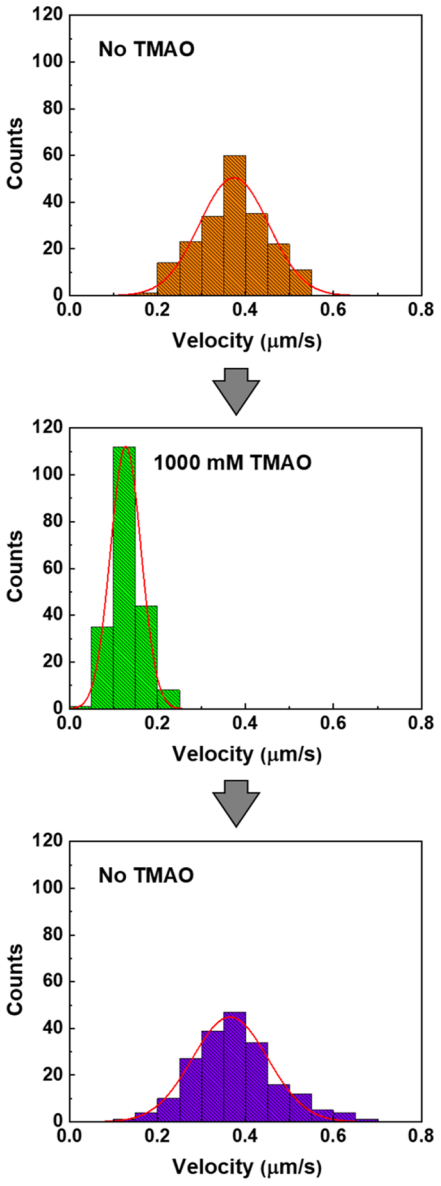

Figure 4. Reversible regulation of the distribution of instantaneous velocity of MTs using TMAO. The distribution of MT velocity in the absence of TMAO (top), in the presence of 1 M TMAO (middle), and after elimination of the TMAO, *i.e.*, in the absence of TMAO (bottom). The red lines represent fitting of the histograms using the equation of Gaussian distribution.

Although, based on our results, TMAO is found useful in controlling the fluctuations in the sliding movement of MTs, the associated mechanism behind such modulation is unclear at this moment. Despite that, defective motors, motor orientation or attachment geometry of motors to MTs, and stiffness of motors have been suspected to play important roles in the fluctuation in the sliding movement of MTs at saturating ATP concentrations. Recently, an increased frequency of pinning of gliding MTs in the presence of TMAO was reported.[39] Pinning of MTs by defective motors is known to increase the motional diffusion coefficient.[23] However, in our

https://doi.org/10.1021/acsomega.2c01228
ACS Omega 2022, 7, 18597−18604

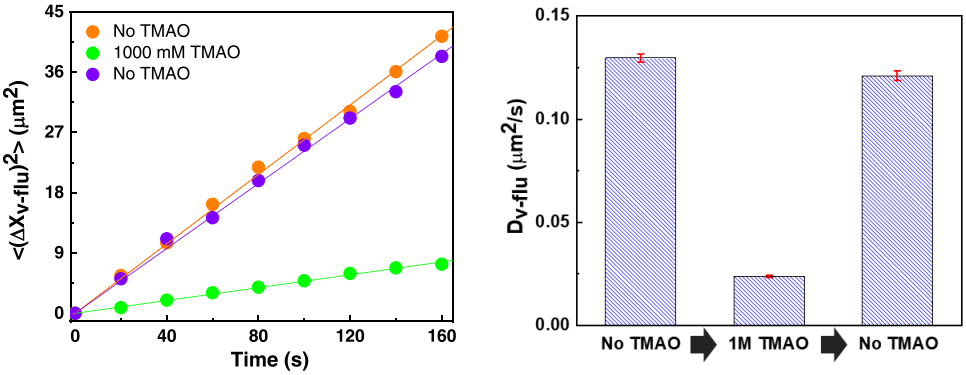

Figure 5. Mean-square displacement deviation of MTs from the average as a function of time, calculated by "multiple trajectories averaging" over 50 different trajectories of MTs, in the absence of TMAO, upon application of 1 M TMAO, and upon elimination of the TMAO (left). Error bars are not shown here for simplicity. The solid lines indicate the linear regression fit of the data in each condition. Reversible regulation of the motional diffusion coefficient of MTs using 1 M TMAO (right). Error bar: standard deviation.

work, we observed a decrease in the motional diffusion coefficient of MTs upon increasing the TMAO concentration in the gliding assay. Moreover, we carefully selected smooth MT trajectories to exclude the effect of MT pinning on our results. Thus, based on these arguments, we can rule out any involvement of pinning of MTs in the altered motional diffusion coefficients of MTs observed in our work. On the other hand, the deep-sea osmolyte TMAO is known to stabilize the biomolecular motor proteins through alteration in their surrounding microenvironments, which is also known to affect the structure of motor proteins.[34] Such alterations in the motor structure may affect the mechanical property, *e.g.*, stiffness of kinesin motors or kinesin's attachment geometry to MTs, which, in turn, may alter the motional diffusion coefficient of MTs in the gliding assay.[40] Further investigation will be required in future to unravel the mechanism behind TMAO-mediated alteration in fluctuations of the motility of the kinesin-propelled MTs.

Although fluctuation of the velocity of the kinesin-propelled MTs has been regulated using TMAO, the velocity of MTs has also been sacrificed in this process. The decreased velocity of MTs may adversely impact their applications; for example, due to the slower velocity of MTs, a relatively longer time would be required to deliver nanomaterials to a target destination. The experimental conditions should be optimized considering a trade-off between MT velocity and fluctuation in their velocity. In this work, we have investigated the dynamic behavior of kinesin-propelled microtubules in the presence of TMAO without sacrificing the fuel (ATP) concentration. Therefore, we maintained a saturating concentration of ATP (5 mM) in our experiments. On the one hand, this strategy will permit using the available ATP for operating any other biomolecular processes together with our presented experimental system of MT−kinesin. On the other hand, use of a high ATP concentration will allow the kinesins to propel MTs for longer time. Considering the emerging applications of biomolecular motors in molecular machine, molecular robotics, micro/nanodevices, synthetic biology, *etc.*, these two advantages would be important. Furthermore, we have performed *in vitro* gliding assay of MTs, in the absence of TMAO, by decreasing the ATP concentration from 5 mM to 50 μM. The average velocity of MTs was 106 ± 18 nm/s using 50 μM ATP, which is close to the velocity of MTs (116 ± 16 nm/s) observed using 1000 mM TMAO and 5 mM ATP. In these conditions, the motional diffusion coefficients of MTs were estimated to be 0.032 ± 0.002 and 0.021 ± 0.001 $\mu m^2/s$ when the average MT velocities were 106 ± 18 nm/s (50 μM ATP, no TMAO) and 116 ± 16 nm/s (5 mM ATP, 1000 mM TMAO), respectively. This result confirms that the suppressed velocity of MTs was not the sole factor in controlling uniformity in MT motion and TMAO plays a direct role as a regulator of dispersion in MT velocity.

Finally, it is to note that we have also performed *in vitro* gliding assay of MTs on kinesin where we decreased the concentration of ATP from 5 to 1 mM, which is still a saturating concentration.[22] Here, the concentration of $MgCl_2$ was 1 mM, whereas the concentration of TMAO was 1000 mM. In this experimental condition, the velocity of MTs was 108 ± 15 nm/s, whereas the velocity of MTs in the absence of TMAO was 313 ± 22 nm/s using 1 mM ATP. This result confirms that the decrease in the gliding velocity of MTs or suppression of fluctuation of the MT velocity in the presence of TMAO, as discussed above, was not due to any decrease in the effective concentration of ATP. It was the TMAO that caused such a decrease in the gliding velocity of MTs, possibly by altering the activity of kinesin motors, confirmation of which requires further investigation in the future.

4. CONCLUSIONS

Utilizing the deep-sea osmolyte TMAO, we have successfully regulated the fluctuation in the sliding movement of kinesin-propelled MTs, in an *in vitro* gliding assay, in a reversible manner. The motional diffusion coefficient of the motile MTs is tuned over a wide range, even at a saturating fuel concentration, simply by varying the concentration of TMAO. Fluctuations in the motility of kinesin-propelled MTs were reported to be affected by the length of MTs and kinesin density on the substrate. However, any report that could offer an efficient strategy to systematically regulate the fluctuations in motility of MTs was lacking. This work provides such a guideline to control the dynamic behavior of the self-propelled biomolecular motor system MT−kinesin. An ability to control the fluctuations in motility of biomolecular motor-propelled shuttles, which is an important design metric in miniaturized lab-on-a-chip devices, is expected to further advance the applications of biomolecular motors in nano-technology, materials science, and other related fields.[41,42]

https://doi.org/10.1021/acsomega.2c01228
ACS Omega 2022, 7, 18597−18604

■ ASSOCIATED CONTENT

Supporting Information

The Supporting Information is available free of charge at https://pubs.acs.org/doi/10.1021/acsomega.2c01228.

Additional experimental results on the effect of TMAO on the standard deviation of the MT velocity and standard deviation/average velocity of MTs, mean-square deviation of the displacement of MTs as a function of travel time at various TMAO concentrations, reversible change of the mean-square deviation of the displacement of MTs as a function of travel time at 1000 mM TMAO, and captions for supporting movies (PDF)

Motility of MTs on kinesins, in an *in vitro* gliding assay, in the absence of TMAO. The field of view is 237.6 μm × 281.6 μm (Movie S1) (MP4)

Motility of MTs on kinesins, in an *in vitro* gliding assay, in the presence of 1200 mM TMAO. The field of view is 237.6 μm × 281.6 μm (Movie S2) (MP4)

■ AUTHOR INFORMATION

Corresponding Authors

Arif Md. Rashedul Kabir − *Faculty of Science, Hokkaido University, Sapporo 060-0810, Japan;* orcid.org/0000-0001-6367-7690; Email: kabir@sci.hokudai.ac.jp

Akira Kakugo − *Faculty of Science, Hokkaido University, Sapporo 060-0810, Japan; Graduate School of Chemical Sciences and Engineering, Hokkaido University, Sapporo 060-0810, Japan;* orcid.org/0000-0002-1591-867X; Email: kakugo@sci.hokudai.ac.jp

Authors

Tasrina Munmun − *Graduate School of Chemical Sciences and Engineering, Hokkaido University, Sapporo 060-0810, Japan*

Kazuki Sada − *Faculty of Science, Hokkaido University, Sapporo 060-0810, Japan; Graduate School of Chemical Sciences and Engineering, Hokkaido University, Sapporo 060-0810, Japan;* orcid.org/0000-0001-7348-0533

Complete contact information is available at: https://pubs.acs.org/10.1021/acsomega.2c01228

Author Contributions

§A.M.R.K. and T.M. contributed equally to this work. A.M.R.K. contributed to conceptualization; A.M.R.K. and A.K. contributed to funding acquisition; T.M. and A.M.R.K. contributed to methodology; T.M. contributed to material preparation and investigation; T.M. and A.M.R.K. contributed to data analysis; A.M.R.K. contributed to project administration and supervision; A.M.R.K. contributed to original draft writing; and A.M.R.K., T.M., K.S., and A.K contributed to review and editing of the manuscript.

Notes

The authors declare no competing financial interest.

■ ACKNOWLEDGMENTS

This work was supported by a research grant (PK22201017) from the Hirose Foundation and JSPS KAKENHI Grant Numbers JP21K04846 and JP20H05972 awarded to A.M.R.K and JSPS KAKENHI Grant Numbers JP18H05423, JP21H04434, and JP21K19877 awarded to A. K.

■ REFERENCES

(1) Phillips, R., Kondev, J., Theriot, J. Dynamics of Molecular Motors. In *Physical Biology of the Cell*, 1st ed.; Morales, M., Ed.; Garland Science: New York, USA, 2009; pp 589−644.

(2) Alberts, B., Bray, D., Watson, J., Lewis, J., Roberts, K., Raff, M. The Cytoskeleton. In *Molecular Biology of the Cell*, 5th ed.; Anderson, M., Granum, S., Eds.; Garland Science: New York, USA, 2007; pp 965−1052.

(3) Howard, J. ATP Hydrolysis. In *Mechanics of Motor Protein and the Cytoskeleton*, 1st ed.; Sinauer Associates Inc.: MA, USA, 2001; pp 229−244.

(4) Vale, R. D.; Fletterick, R. J. The design plan of kinesin motors. *Annu. Rev. Cell Dev. Biol.* **1997**, *13*, 745−777.

(5) Kirschner, M.; Mitchison, T. Beyond self-assembly: from microtubules to morphogenesis. *Cell* **1986**, *45*, 329−342.

(6) van den Heuvel, M. G. L.; Dekker, C. Motor proteins at work for nanotechnology. *Science* **2007**, *317*, 333−336.

(7) Jia, Y.; Li, J. Molecular assembly of rotary and linear motor proteins. *Acc. Chem. Res.* **2019**, *52*, 1623−1631.

(8) Hess, H. Engineering applications of biomolecular motors. *Annu. Rev. Biomed. Eng.* **2011**, *13*, 429−450.

(9) Harada, Y.; Noguchi, A.; Kishino, A.; Yanagida, T. Sliding movement of single actin filaments on one-headed myosin filaments. *Nature* **1987**, *326*, 805−808.

(10) Toyoshima, Y. Y.; Kron, S. J.; Spudich, J. A. The myosin step size: measurement of the unit displacement per ATP hydrolyzed in an in vitro assay. *Proc. Natl. Acad. Sci.* **1990**, *87*, 7130−7134.

(11) Uyeda, T. Q.; Abramson, P. D.; Spudich, J. A. The neck region of the myosin motor domain acts as a lever arm to generate movement. *Proc. Natl. Acad. Sci.* **1996**, *93*, 4459−4464.

(12) Fischer, T.; Agarwal, A.; Hess, H. A smart dust biosensor powered by kinesin motors. *Nat. Nanotechnol.* **2009**, *4*, 162−166.

(13) Bachand, G. D.; Rivera, S. B.; Boal, A. K.; Gaudioso, J.; Liu, J.; Bunker, B. C. Assembly and transport of nanocrystal CdSe quantum dot nanocomposites using microtubules and kinesin motor proteins. *Nano Lett.* **2004**, *4*, 817−821.

(14) Bachand, G. D.; Rivera, S. B.; Carroll-Portillo, A.; Hess, H.; Bachand, M. Active capture and transport of virus particles using a biomolecular motor-driven, nanoscale antibody sandwich assay. *Small* **2006**, *2*, 381−385.

(15) Hess, H.; Clemmens, J.; Howard, J.; Vogel, V. Surface imaging by self-propelled nanoscale probes. *Nano Lett.* **2002**, *2*, 113−116.

(16) Inoue, D.; Nitta, T.; Kabir, A. M. R.; Sada, K.; Gong, J. P.; Konagaya, A.; Kakugo, A. Sensing surface mechanical deformation using active probes driven by motor proteins. *Nat. Commun.* **2016**, *7*, No. 12557.

(17) Hess, H.; Howard, J.; Vogel, V. A piconewton forcemeter assembled from microtubules and kinesins. *Nano Lett.* **2002**, *2*, 1113−1115.

(18) Keya, J. J.; Suzuki, R.; Kabir, A. M. R.; Inoue, D.; Asanuma, H.; Sada, K.; Hess, H.; Kuzuya, A.; Kakugo, A. DNA-assisted swarm control in a biomolecular motor system. *Nat. Commun.* **2018**, *9*, No. 453.

(19) Liu, H.; Schmidt, J. J.; Bachand, G. D.; Rizk, S. S.; Looger, L. L.; Hellinga, H. W.; Montemagno, C. D. Control of a biomolecular motor-powered nanodevice with an engineered chemical switch. *Nat. Mater.* **2002**, *1*, 173−177.

(20) Konishi, K.; Uyeda, T. Q.; Kubo, T. Genetic engineering of a Ca^{2+} dependent chemical switch into the linear biomotor kinesin. *FEBS Lett.* **2006**, *580*, 3589−3594.

(21) Amrutha, A. S.; Kumar, S. K. R.; Tamaoki, N. Azobenzene-based photoswitches facilitating reversible regulation of kinesin and myosin motor systems for nanotechnological applications. *ChemPhotoChem* **2019**, *3*, 337−346.

(22) Böhm, K. J.; Stracke, R.; Unger, E. Speeding up kinesin-driven microtubule gliding in vitro by variation of cofactor composition and physicochemical parameters. *Cell Biol. Int.* **2000**, *24*, 335−341.

(23) Nitta, T.; Hess, H. Dispersion in active transport by kinesin-powered molecular shuttles. *Nano Lett.* **2005**, *5*, 1337−1342.

(24) Imafuku, Y.; Toyoshima, Y. Y.; Tawada, K. Fluctuation in the microtubule sliding movement driven by kinesin in vitro. *Biophys. J.* **1996**, *70*, 878−886.
(25) Kelly, R. H.; Yancey, P. H. High contents of trimethylamine oxide correlating with depth in deep-sea teleost fishes, skates, and decapod crustaceans. *Biol. Bull.* **1999**, *196*, 18−25.
(26) Yancey, P. H.; Clark, M. E.; Hand, S. C.; Bowlus, R. D.; Somero, G. N. Living with water stress: evolution of osmolyte systems. *Science* **1982**, *217*, 1214−1222.
(27) Lidbury, I.; Murrell, J. C.; Chen, Y. Trimethylamine N-oxide metabolism by abundant marine heterotrophic bacteria. *Proc. Natl. Acad. Sci.* **2014**, *111*, 2710−2715.
(28) Bachand, G. D.; Jain, R.; Ko, R.; Bouxsein, N. F.; VanDelinder, V. Inhibition of microtubule depolymerization by osmolytes. *Biomacromolecules* **2018**, *19*, 2401−2408.
(29) Chase, K.; Doval, F.; Vershinin, M. Enhanced stability of kinesin-1 as a function of temperature. *Biochem. Biophys. Res. Commun.* **2017**, *493*, 1318−1321.
(30) Castoldi, M.; Popov, A. V. Purification of brain tubulin through two cycles of polymerization−depolymerization in a high-molarity buffer. *Protein Expression Purif.* **2003**, *32*, 83−88.
(31) Peloquin, J.; Komarova, Y.; Borisy, G. Conjugation of fluorophores to tubulin. *Nat. Methods* **2005**, *2*, 299−303.
(32) Fujimoto, K.; Kitamura, M.; Yokokawa, M.; Kanno, I.; Kotera, H.; Yokokawa, R. Colocalization of quantum dots by reactive molecules carried by motor proteins on polarized microtubule arrays. *ACS Nano* **2013**, *7*, 447−455.
(33) Munmun, T.; Kabir, A. M. R.; Sada, K.; Kakugo, A. Complete, rapid and reversible regulation of the motility of a nano-biomolecular machine using an osmolyte trimethylamine-N-oxide. *Sens. Actuators, B* **2020**, *304*, No. 127231.
(34) Kumemoto, R.; Yusa, K.; Shibayama, T.; Hatori, K. Trimethylamine N-oxide suppresses the activity of the actomyosin motor. *Biochim. Biophys. Acta, Gen. Subj.* **1820**, *2012*, 1597−1604.
(35) Qian, H.; Sheetz, M. P.; Elson, E. L. Single particle tracking. Analysis of diffusion and flow in two-dimensional systems. *Biophys. J.* **1991**, *60*, 910−921.
(36) Tawada, K.; Sekimoto, K. Protein friction exerted by motor enzymes through a weak-binding interaction. *J. Theor. Biol.* **1991**, *150*, 193−200.
(37) Bormuth, V.; Varga, V.; Howard, J.; Schäffer, E. Protein friction limits diffusive and directed movements of kinesin motors on microtubules. *Science* **2009**, *325*, 870−873.
(38) Munmun, T.; Kabir, A. M. R.; Katsumoto, Y.; Sada, K.; Kakugo, A. Controlling the kinetics of interaction between microtubules and kinesins over a wide temperature range using the deep-sea osmolyte trimethylamine N-oxide. *Chem. Commun.* **2020**, *56*, 1187−1190.
(39) VanDelinder, V.; Sickafoose, I.; Imam, Z. I.; Ko, R.; Bachand, G. D. The effects of osmolytes on in vitro kinesin-microtubule motility assays. *RSC Adv.* **2020**, *10*, 42810−42815.
(40) Palacci, H.; Idan, O.; Armstrong, M. J.; Agarwal, A.; Nitta, T.; Hess, H. Velocity fluctuations in kinesin-1 gliding motility assays originate in motor attachment geometry variations. *Langmuir* **2016**, *32*, 7943−7950.
(41) Tsitkov, S., Hess, H. Design of active nanosystems incorporating biomolecular motors. In *Out-of-Equilibrium (Supra) molecular Systems and Materials*, 1st ed.; Giuseppone, N., Walther, A., Eds.; Wiley-VCH: Weinheim, Germany, 2021; pp 379−422.
(42) Saper, G.; Hess, H. Synthetic systems powered by biological molecular motors. *Chem. Rev.* **2020**, *120*, 288−309.

https://doi.org/10.1021/acsomega.2c01228
ACS Omega 2022, 7, 18597−18604